



## ISTITUTO NAZIONALE DI RICERCA METROLOGICA Repository Istituzionale

Measuring the impact of reversible substations on energy efficiency in rail transport

*Original*

Measuring the impact of reversible substations on energy efficiency in rail transport / Cascetta, F.; Cipolletta, G.; Delle Femine, A.; Gallo, D.; Giordano, D.; Signorino, D.. - (2020), pp. 123-128.

*Availability:*

This version is available at: 11696/66575 since: 2021-02-05T17:46:44Z

*Publisher:*

*Published*

DOI:

*Terms of use:*

This article is made available under terms and conditions as specified in the corresponding bibliographic description in the repository

*Publisher copyright*

(Article begins on next page)

# Measuring the impact of reversible substations on energy efficiency in rail transport.

F. Cascetta<sup>1</sup>, G. Cipolletta<sup>1</sup>, A. Delle Femine<sup>1</sup>,  
D. Gallo<sup>1</sup>, D. Giordano<sup>2</sup>, D. Signorino<sup>2</sup>

<sup>1</sup> *University of Campania "Luigi Vanvitelli" Aversa (CE), Italy, giuliano.cipolletta@unicampania.it*

<sup>2</sup> *Italian National Institute of Metrological Research (INRIM) Torino, Italy, d.signorino@inrim.it*

**Abstract** – Nowadays great interest is placed on the environmental issue. Greenhouse gas emissions are more than 50% higher than in 1990. European energy policy has been supporting efficient energy management in order to reduce the railway transport emissions by 50% within 2030. The railway stakeholders are encouraged to adopt technological solutions to foster energy efficiency. The electrodynamic braking combined with the adoption of reversible substations is one of the most promising solutions. In order to evaluate the impact of this innovative technology, a measurement campaign has been conducted on Metro de Madrid where a reversible substation was installed. In this paper, a preliminary analysis on the data acquired is presented. Traceable and accurate on-board train measurements of the energy flows and the losses are fundamental to quantify the impact of these new technologies and to carry out a survey on the efficiencies of the different vehicle components and on the strategies to reduce the energy consumption in the various operation modes.

## I. INTRODUCTION

The transportation impacts significantly on the global energy demand. In order to reduce the dependency of world from fossil fuel, not necessarily reducing human activity, it is possible to make more efficient use of energy resources.

The electric railway systems have significant advantages in terms of energy efficiency and absence of local emissions, compared with other means of transportation. As one of the most sustainable and safest modes of transport we have, rail will play a major role in Europe's future mobility system.

The EU Commission, with the European Strategy "Transport 2050", has outlined a competitive transport system, able to increase mobility and reduce carbon dioxide emissions in transport by 60% by 2050, not only for environmental reasons but also to reduce oil imports (Directive 2014/94/EU also called DAFI, Alternative Fuel Infrastructure Directive) [1], [2].

The strategy sets different goals for different types of travel behaviors within cities. One of its key goals is to achieve carbon-free movement in major urban centers by 2030. The initiative also includes encouraging a shift towards public transport and bringing the number of road fatalities to zero by 2050. The strategy also aims for a 50 percent shift of intercity

passengers who travel 300 km or more from road to rail.

Rail is not only environmentally friendly and energy-efficient, but it is also the only mode of transport to have almost continuously reduced its CO<sub>2</sub> emissions since 1990, at the same time as it increased transport volumes. Nevertheless, the total amount of energy required for the European railway system is a huge number (78,9 TWh for EEA33 excluding Switzerland and Liechtenstein in 2018, source Eurostat) and the growing need of vehicles with a higher on-board comfort and, in turn, higher transport capacity entails a growing demand for traction energy. In order to achieve the ambitious targets fixed by the European policy in terms of emissions and simultaneously to cope with increasing traffic demand, energy efficiency of railway system must be considerably enhanced. Furthermore, given the highly competitive context of the other modes of urban transportation, a reduction in energy consumption is crucial for the rail to keep its competitiveness as the most sustainable and economic means of transport [1].

Among the main technical solutions that can foster the energy efficiency of electric railway systems, the recovering of kinetic energy during the braking [3] is the most promising one. In principle, when an electric vehicle brakes, it could invert its electric motor control, so its motors work as generators converting the kinetic energy back in the electric form. This is called electrodynamic braking (alternative to the traditional mechanic braking that instead wastes the kinetic energy), [4]. This recovered energy can be consumed on-board (by auxiliary systems for example) or reinjected on the over-head line. In DC railway systems, the common supply substations allow only a unidirectional energy flow (from the electrical grid to the trains) so the regenerated energy, once injected on the catenary, can be only reused by other adjacent trains that need energy in that specific moment on the same section of track. If this condition does not occur, the energy should be dissipated on board by dedicated rheostats to avoid excessive increasing of catenary voltage level [5]-[7]. Nevertheless, there is only a certain probability of having simultaneously one train braking and another accelerating on the same line, so at present, a considerable amount of this energy is dissipated.

A solution to increase energy saving from braking is the adoption of energy storage devices installed near the railway line. Since the braking energy presents high power peaks for short time, one of the best solutions to this scope are

supercapacitor banks. But with available energy density they require a lot of space for their installation and dedicated power electronic converters to adapt the system voltage to the storage voltage and to manage the reutilization of energy within a short time, in order to avoid self-discharge and maintain high efficiency. Moreover, their management and their sizing are not simple tasks. Alternatively, this energy could be stored on-board. Nevertheless, storing this surplus of energy would require high maintenance costs and increase the weight of the rolling stocks, with negative consequence on the overall efficiency, [8].

The introduction of reversible substations could solve this issue, greatly improving the line receptivity. With this technological innovation, the regenerated energy, not absorbed by other trains, could be instead returned to the AC power distribution network, making it available for other AC loads and potentially sold to the energy provider. Obviously, this option requires significant investments by the railway stakeholders as it should be necessary to substitute all the energy converters with modern bidirectional ones.

For an economic assessment, it is necessary to have a reliable quantification of the energy that can be saved by adopting this technique, but at present these data are not available. In order to have a complete and accurate knowledge of the energy fluxes of a real metro service during normal working conditions, and so quantifying the impact of the installation of new reversible substations from both points of view environmental and economic, a specific measurement system was developed. This activity is part of the metrology research project EMPIR 16ENG04 MyRailS [9], [10], [11].

This system was installed on board a train operating on a metro line in the city of Madrid, where a reversible substation was installed. At the best author knowledge, at the moment of writing, this is the first time that such a research is conducted on a subway line with bidirectional supply system. In the following, in Section II the line and train subject of the research will be illustrated. Section III describes measurement system together with the measurement points. Experimental results with numerical analysis and some authors' considerations on the preliminary data will be reported in section IV.

## II. SUBWAY LINE AND TRAIN UNDER ANALYSIS

To reduce management costs and the ecological footprint of the metro of Madrid, one of the substations was modified adding a DC/AC converter of 2 MW in anti-parallel to a traditional, already present rectifier of 3 MW. In this way, a bidirectional flow of energy was obtained with minimal modification of the existing electric system.

This DC/AC converter has been installed at the substation of La Moraleja located in the middle of the line 10B that goes from Hospital Infanta Sofia to Tres Olivos with 11 stations (see Fig. 1). The line covers a distance of about 15 km and the roundtrip journey lasts about 47 minutes. The analysis was conducted taking as reference a common train in normal operation on that line. It is a subway train with three cars, model "S9000 3 CARS SS3" (see Fig.2), whose main characteristics are reported in Table 1. From the electrical point of view, the nominal line voltage of the train is 1500 V DC and the maximum current absorption is of 1650 A.

The train under test has two locomotives, with two traction



Fig. 1. The 11 stops of the line 10B.



Fig. 2. Train under test

systems and two independent pantographs. The two traction units are controlled with identical commands and they work in nearly the same conditions, so it is possible to assume that energy flows are nearly identical.

Therefore, it was decided to install the monitoring system on a single locomotive (called half train) so, in the following, all the discussion and results will be referred to a single traction unit, namely a half train. But to obtain an evaluation of power and energy absorbed by the whole train, it is possible to simply scale by two the values obtained by the single traction carriage.

Fig.3 reports a simplified diagram of the input stage of the monitored locomotive. The energy absorbed by the pantograph is divided between two loads: the traction energy, that represents the main load, and the auxiliary services, which consists of the sum of all the other loads on board (air conditioner, illumination, electric door, and other electric and electronic on board systems).

Table 1. General characteristics of trains S9000

Parameter	Value
Total lenght	54 m
CarM length	18.550 m
CarR length	17.800 m
Axle	12
Rated supply voltage	1500 V
Total power	8 x 187 kW
Maximum car height	3.878 m
Car width	2.808 m
Total weight	95000 kg
Maximum speed	110 km/h

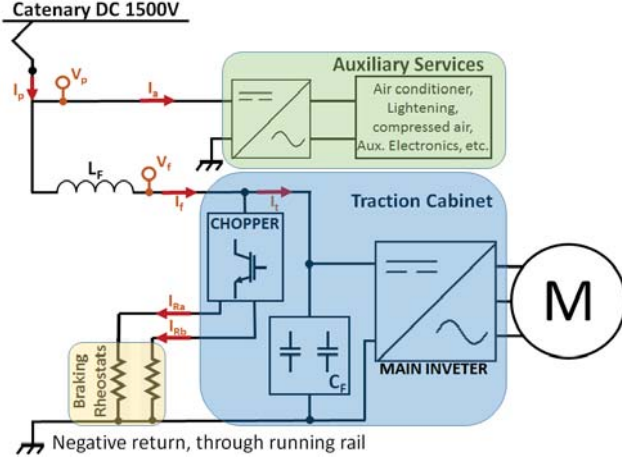


Fig. 3. Electric diagram of the traction carriage of S9000.

The inductance  $L_F$  and the capacitor bank  $C_F$  compose a second order filter necessary to limit the voltage distortion coming from the line ( $V_p$ ) to the inverter ( $V_t$ ), and, at the same time, to limit the current distortion injected by the inverter in the supply line. Like stated before, the capability of the over-head line to absorb the power generated by a train, during the dynamic braking, depends on the presence of other trains on the same line.

Obviously, during a dynamic braking, the voltage after the filter ( $V_t$ ) increases. When the injection of current into supply system is not possible, a chopper supplying two resistors is adopted to dissipate on board the electrical energy generated during a braking phase.

The current in the rheostats,  $I_{Ra}$  and  $I_{Rb}$ , can be regulated so it is possible to regulate the ratio between the amount of energy wasted locally and that injected in the overhead contact line. The control variable for this process is  $V_t$ : when it exceeds 1700 V the chopper begins to gradually increase the dissipation on board so decreasing the current injected in the supply line and thus reducing the voltage to the normal operating range. The current directed to the resistors is Pulse Width Modulated (PWM). The average values of the currents  $I_{Ra}$  and  $I_{Rb}$  are regulated by the duty cycle of PWM pulses. The frequency of PWM modulation is at about 300 Hz, the peak amplitude is 600 A and the duty cycle varies from 2% to a maximum of 50%. This can lead to current pulses that can last as little as 66  $\mu$ s.

### III. MEASUREMENT SETUP

To have a complete knowledge of energy fluxes of the train during all operating conditions, the monitored quantities are (see Fig. 3):  $V_p$ , that is the common voltage for traction and auxiliary systems, and  $V_t$ , that is the voltage applied on the two braking rheostats  $I_p$ , that is the total current,  $I_t$ , that is the traction cabinet input current,  $I_a$ , that is the auxiliary systems current and  $I_{Ra}$  with  $I_{Rb}$ , that are the currents in the braking rheostats. The energy exchange is mainly at low frequency (basically DC) but, for more insight analyses, large bandwidth instrumentations are required for instance to measure the chopped currents in the rheostats or the fast transients that can occur at the pantograph (e. g. arc events [10]).

To this aim, a proper measurement system able to acquire and to store two voltages and five currents, was developed (see

Fig. 4). It is based on a National Instruments Compact Rio 9034 that is a stand-alone reconfigurable embedded chassis, that features an embedded controller with a 1.91 GHz real time processor, a reconfigurable (field Programmable Gate Array) FPGA, 2 GB RAM DDR3 and a SD port for data storage. As regards the acquisition modules, the Compact Rio houses two NI 9223 that are 4-channel voltage modules, with differential inputs and simultaneous sampling with a maximum range of  $\pm 10$  V, 1 MHz as maximum sampling rate and a resolution of 16 bit. The data acquisition is performed at a sample rate of 50 kHz. The acquisition system is referenced to absolute time via the GPS module NI 9467, that provides a Pulse Per Second (PPS) signal with an accuracy of 100 ns. Obviously, the GPS receiver cannot work well underground, but the train passes in an open sky track at least once a day, the system can synchronize with UTC in that moment and then it keeps time using internal real time clock until next synchronization. Furthermore, the NI 9211 thermocouple input module (with 14 Samples/s Aggregate,  $\pm 80$  mV of input range, 24 bit delta sigma analog to digital converter, anti-aliasing filter, open thermocouple detection and cold junction compensation for high accuracy thermocouple measurement) has been employed to monitor the temperature inside the rheostats room.

Two Ultravolt 40TF-CDCD (40 kV/40 V 0 Hz  $\div$  1 MHz, 0.25 %) resistive-capacitive compensated dividers have been adopted to scale down the voltages  $V_p$ , and  $V_t$  which nominal amplitude is 1500 V. Open loop Hall effect current transformers have been used for the currents. They have openable magnetic core, that facilitate the installation on-board train. Two different models have been used, the HOP 2000 and the HOP 800 from LEM respectively with 2000 A and 800 A of primary nominal current. The first has been used for  $I_p$  and  $I_t$ , which amplitudes can reach 1000 A. The second instead is used for  $I_a$ ,  $I_{Ra}$  and  $I_{Rb}$  as they reach significantly lower amplitudes (600 A for  $I_{Ra}$  and  $I_{Rb}$ , less than one hundred ampere for  $I_a$ ). Both models feature an accuracy better than 2 % and a flat frequency response from DC to 10 kHz. The measurement system and the transducers are battery powered in order to allow a continuous monitoring of the train signals, even when the pantograph is not in contact with the catenary.

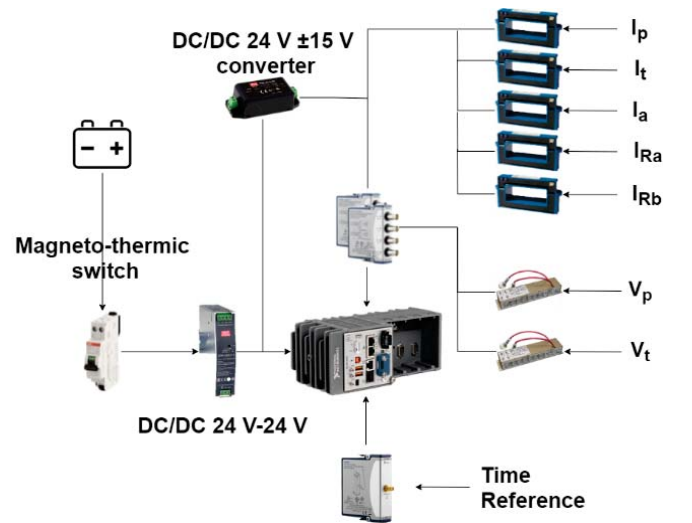


Fig. 4. Measurement setup.

The data acquisition system has been located in the low voltage cabinet. The voltage divider related to the pantograph voltage measurement and the current transducer related to the auxiliary service current have been installed in the high voltage cabinet. The other transducers are located under the train in proximity of the traction cabinet. All the transducers adopted have been metrologically characterized at INRIM laboratories to guarantee traceability. The calibrations were carried out in stationary conditions at various levels of amplitude. DC gains and offsets were accurately assessed with an expanded uncertainty of 10 ppm for voltage and 50 ppm for current, both gain and offset, with a confidence level of approximately 95 % ( $k = 2$ ). All subsequent measurements were compensated using the calibration results [12].

To evaluate the DC energy flows in the different working conditions of the train, a preliminary analysis has been conducted with acquired signals averaged on  $\Delta T = 1$  s.

From basic current balance, see Fig. 3, it results:

$$I_p = I_a + I_f = I_a + I_R + I_t \quad (1)$$

where in the considered measurement system, the value of  $I_t$  have been evaluated indirectly with the relation:

$$I_t = I_f - I_R \quad (2)$$

and  $I_R$  is the total current dissipated in the rheostats given by:

$$I_R = I_{Ra} + I_{Rb} \quad (3)$$

The balance of the DC energies results:

$$E_p = E_a + E_L + E_t + E_R \quad (4)$$

where  $E_p$  is the total energy absorbed at pantograph,  $E_a$  is the energy absorbed by auxiliary systems,  $E_L$  is the energy dissipated in the input filter,  $E_t$  is the energy absorbed by traction system and  $E_R$  is the energy dissipated by the braking rheostats. To obtain these energies from the average values of monitored voltages and currents, it is possible at first to calculate the corresponding DC power in each  $\Delta T$  as:

$$P_p = V_p I_p; \quad P_a = V_p I_a; \quad (5)$$

$$P_L = I_f (V_p - V_f); \quad (6)$$

$$P_t = V_f I_t = V_f (I_f - I_R); \quad (7)$$

$$P_R = V_f I_R = V_f (I_{Ra} + I_{Rb}); \quad (8)$$

then to multiply these values for  $\Delta T$  and to sum all the values of the considered time interval.

During acceleration intervals ( $I_t > 0$ ),  $E_r$  (and  $I_R$ ) is equal to zero and all the other quantities in (4) are positive. Almost all of current goes for traction (the currents of the auxiliary services and the rheostats are limited). During the brake, the energy flux is inverted:  $E_t$  becomes negative (energy is generated by the motors) and, depending on the line receptivity, the energy could be dissipated in the braking rheostats ( $E_R > 0$ ) or injected in the supply system ( $E_p < 0$ ). It is also possible that the generated energy is partially injected and partially dissipated: in fact, in (4)  $E_a$  and  $E_L$  are always positive so  $E_p$  is negative or zero as a consequence of the amount of dissipated energy ( $E_R$ ).

#### IV. EXPERIMENTAL RESULTS

The measurement campaign has been started on the October 2019 and the system is still installed but the activities are at moment suspended for the worldwide sanitary emergency due to Covid-19. Nevertheless, eighteen days of continuous acquisition have been performed, during which more than 350 of roundtrip journeys have been monitored and about 500 GB of data have been stored.

In Fig. 5 the traction current obtained by (2) is reported as example of a typical journey from Hospital Infanta Sofia to Tres Olivos. The time intervals corresponding to the ten movements of the train between consecutive stations (sub-tracks) are evidenced: it is possible to recognize the acceleration stages leaving from the stations (big positive current spikes) and the brake stages approaching to the next stations (big negative current spikes). After the braking, the train stops ( $I_t$  goes almost to zero) for a while in each station before leaving again. The movement of the train was not always regular and sometimes had to brake before approaching the station, probably either approaching a bend or, alternatively, due to the presence of another train that had not yet left the next station (see Fig. 5 sub-track 4 – 8, starting from the first green dashed line). In the last part there is a speed limitation that consequently also limits the current absorption.

During all the brakes the train tries to inject energy in the supply system but, as previously stated, this energy injection firstly depends on the presence of a contemporary absorption (traction) of some other trains on the same line. If this lucky condition does not apply, the regenerated energy should be transferred to the reversible substation. When the supply line had not the capability to absorb all the generated energy, the excess part must be dissipated on board the train by the rheostats. This depends on the state of the other trains (e. g. other regenerative braking at the same time) or from the general dynamic state of the supply line (e.g. distance from regenerative substation or distance from other trains). The lack of receptivity of the supply line was detected by an excessive increment of the supply voltage that triggers the on-board dissipation. Anyway, in the considered installation, almost all the recovered energy is expected to be accepted by the line.

To show an example of this phenomenon, Fig. 6 reports the time evolution of the main electrical signals involved in a typical braking. The reported values are averaged over 0.01 s that is enough for dynamic of almost all signals, except for  $I_R$  (red line) that is reported at 50 kHz.

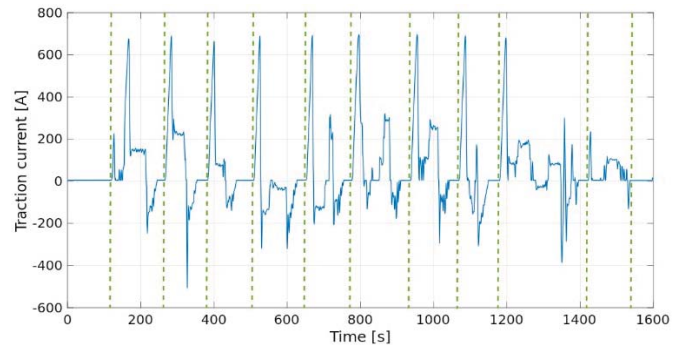


Fig. 5. Traction current ( $I_t$ ) during a one-way trip.

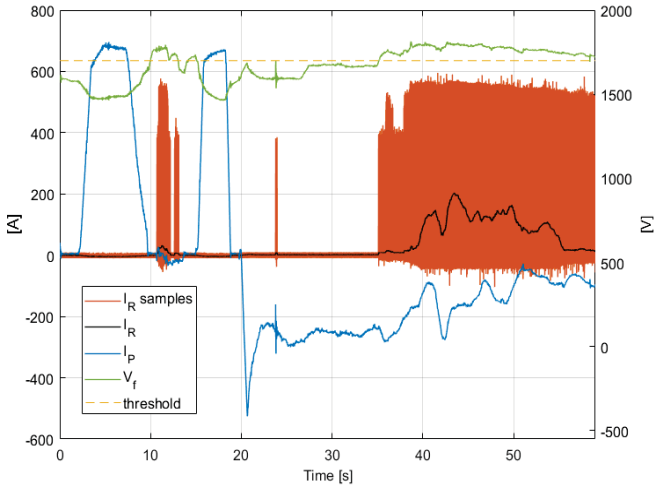


Fig. 6. Energy analysis of braking.

Approximately at second 20 the strong brake starts ( $I_p < 0$ ) with a complete recovery ( $I_R = 0$ ). But at second 35 the level of  $V_f$  overcomes the threshold of 1700 V and chopper starts the dissipation ( $I_R \neq 0$ , red line). Looking at  $I_R$ , it is evident that a remarkable amount of energy is dissipated on-board. This energy is not constant in time. In fact, even if the peak levels of current are nearly constant ( $I_{R \text{ sample}}$  red line), the average value of  $I_R$  (black line) depends on the duty cycle of the chopper. This is not appreciable with instantaneous values graph. The black line shows how the amount of energy changes in agreement with the line receptivity to limit  $V_f$  increasing.

In Table 2 the results of a comprehensive energy analysis of the first week monitored is reported. As stated before, the measurements are conducted on single traction unit, so they should be doubled to have the values for all the train. At the pantograph the absorbed ( $I_p > 0$ ) and the injected ( $I_p < 0$ ) energies are evaluated separately and reported together with the net amount of energy. The average value of the recovery factor was about 38%. During braking stage, as expected, most of the energy is recovered; nevertheless, an average amount of 9% of regenerated energy is dissipated on board. The auxiliary services have a minor impact on energy balance, and they just cover the 5% of the absorbed power. The loss in the input filter (2%) has low influence too.

It is possible to follow the average flows of power during

traction and during brake averaging different energies over working hours (see Fig. 7). The half train works as a load with an average power absorption of about 105 kW. During acceleration periods ( $E_p > 0$ ), almost all the power goes for traction (the auxiliary absorption and filter dissipation gives limited contribute)  $E_R$  is equal to zero. During the brake, the energy flux is inverted:  $E_t$  becomes negative (the energy is generated by the motor) and, as a consequence of the line receptivity, the energy is partially dissipated in the braking rheostats (9%) and partially reused (91%). It is interesting to note that the recovered energy is partially absorbed by auxiliary systems, partially dissipated in the filter and the rest of the energy is fed back to the catenary.

## V. CONCLUSION

As regards the environment and the energy efficiency, rail transport has always stood out for being among the most efficient means of transport. In this article, it has been observed that there is still a lot of operating margin to intervene on these energy-consuming systems. Preliminary result, coming from the energy analysis, show that reversible substation adoption has potential to considerably improve the overall efficiency.

## ACKNOWLEDGMENT

The result here presented are developed in the framework of the 16ENG04 MyRails Project [11], [13] funded by the EMPIR program (European Metrology Program for Innovation and Research) co-financed by the Participating States and the European Union's Horizons 2020 research program.

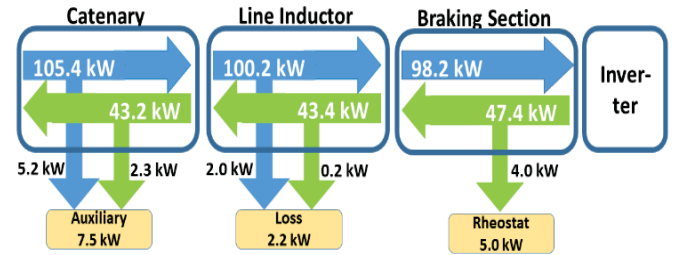


Fig. 7. Average power flows on single traction unit.

Table2. Energy monitoring results

Date	Working hours	number of routes	Input energy (kWh)			Braking energy (kWh)			Auxiliary Services (kWh)			Input filter (kWh)		
			Absorbed	Injected	Net Absorbed	Generated	Dissipated	Net Recovered	Total	Braking Phase	Traction Phase	Total	Braking Phase	Traction Phase
4 - oct	20:46	27	2266	-857	1408	984.63	65	920	206	54	151	46	5	41
5 - oct	20:44	26	2124	-816	1308	946.09	84	862	117	35	82	49	4	44
6 - oct	16:36	21	1626	-613	1013	702.72	52	650	134	33	101	34	3	30
7 - oct	12:45	16	1366	-549	817	623.60	45	578	79	25	54	30	3	27
10 - oct	04:38	6	471	-194	277	214.81	11	204	24	9	15	9	1	8
11 - oct	20:18	26	2264	-919	1344	1064.68	96	969	119	43	76	51	6	45
12 - oct	9:25	12	1037	-385	652	474.67	62	413	92	27	65	22	2	20
15 - oct	16:26	21	1680	-635	1044	753.80	77	677	141	54	88	34	4	31

## REFERENCES

- [1] COM (2011) 144 Wight Paper: Roadmap to a Single European Transport Area – Towards a competitive and resource efficient transport system.
- [2] Directive 2014/94/EU of the European Parliament and of the Council of 22 October 2014 on the deployment of alternative fuels infrastructure.
- [3] Z. Tian, G. Zhang, N. Zhao, S. Hillmanssen, P. Tricoli, C. Roberts "Energy Evaluation for DC Railway Systems with Inverting Substations," *2018 IEEE Intern. ESARS-ITEC Conference*, Nottingham, 2018, pp. 1-6.
- [4] M. Dominguez, A. Fernandez, A. Cucala, R. Pecharroman, "Energy Savings in Metropolitan Railway Substations Through Regenerative Energy Recovery and Optimal Design of ATO Speed Profiles," in *IEEE Transactions on Automation Science and Engineering*, 2012.
- [5] Y. Oura, Y. Mochinaga, H. Nagasawa, "Railway Electric Power Feeding Systems", Japan Railway & Transport Review 16, June 1998.
- [6] A. Delle Femine, D. Gallo, C. Landi, M. Luiso, Discussion on DC and AC power quality assessment in railway traction supply systems (2019) I2MTC 2019 - 2019 IEEE International Instrumentation and Measurement Technology Conference, Proceedings, 2019-May, art. no. 8826869
- [7] IEC 62313:2009 Railway applications - Power supply and rolling stock - Technical criteria for the coordination between power supply (substation) and rolling stock.
- [8] M. Brenna, F. Foiadelli, D. Zaninelli, "Electrical Railway Transportation Systems", Mar 2018, Wiley-IEEE Press.
- [9] D. Giordano, P. Clarkson, F. Garnacho, H.E. van der Brom, L. Donadio, A. Fernandez-Cardador, C. Spalvieri, D. Gallo, D. Istrate, A. De Santiago Laporte, A. Mariscotti, C. Mester, N. Navarro, M. Porzio, A. Roscoe, M. Sira "Accurate Measurements of Energy, Efficiency and Power Quality in the Electric Railway System", CPEM 2018.
- [10] G. Crotti, A. Delle Femine, D. Gallo, D. Giordano, C. Landi, M. Luiso, A. Mariscotti, P. Roccato "Pantograph-to-OHL Arc: Conducted Effects in DC Railway Supply System", IEEE Transactions on Instrumentation and Measurement, 2019.
- [11] EURAMET Joint Research Program "Metrology for Smart Energy Management in Electric Railway Systems" 16ENG04 MyRailsProject.
- [12] G. Crotti, D. Gallo, D. Giordano, C. Landi, M. Luiso, Industrial Comparator for Smart Grid Sensor Calibration (2017) IEEE Sensors Journal, 17 (23), art. No. 7971905, pp. 7784-7793
- [13] A. Delle Femine, D. Gallo, D. Giordano, C. Landi, M. Luiso, D. Signorino, "Power Quality Assessment in Railway Traction Supply Systems", 2020 IEEE Transactions on Instrumentation and Measurement, 69(5), 8962225, pp. 2355-2366